

## Structural Features That Modulate the Transmembrane Migration of a Hydrophobic Peptide in Lipid Vesicles

Sajith Jayasinghe, Melissa Barranger-Mathys, Jeffrey F. Ellena, Craig Franklin, and David S. Cafiso

Department of Chemistry and Biophysics Program at the University of Virginia, Charlottesville, Virginia 22901 USA

**ABSTRACT** Two approaches employing nuclear magnetic resonance (NMR) were used to investigate the transmembrane migration rate of the C-terminal end of native alamethicin and a more hydrophobic analog called L1. Native alamethicin exhibits a very slow transmembrane migration rate when bound to phosphatidylcholine vesicles, which is no greater than  $1 \times 10^{-4} \text{ min}^{-1}$ . This rate is much slower than expected, based on the hydrophobic partition energies of the amino acid side chains and the backbone of the exposed C-terminal end of alamethicin. The alamethicin analog L1 exhibits crossing rates that are at least 1000 times faster than that of native alamethicin. A comparison of the equilibrium positions of these two peptides shows that L1 sits  $\sim 3\text{--}4 \text{ \AA}$  deeper in the membrane than does native alamethicin (Barranger-Mathys and Cafiso, 1996. *Biochemistry*, 35:489). The slow rate of alamethicin crossing can be explained if the peptide helix is irregular at its C-terminus and hydrogen bonded to solvent or lipid. We postulate that L1 does not experience as large a barrier to transport because its C-terminus is already buried within the membrane interface. This difference is most easily explained by conformational differences between L1 and alamethicin rather than differences in hydrophobicity. The results obtained here demonstrate that side-chain hydrophobicity alone cannot account for the energy barriers to peptide and protein transport across membranes.

### INTRODUCTION

Alamethicin is a small 20-amino acid peptide that produces voltage-dependent conductances in planar bilayers and in lipid vesicles (Latorre and Alvarez, 1981; Mathew and Balaram, 1983; Woolley and Wallace, 1992; Cafiso, 1994; Hall et al., 1984; Sansom, 1993). Because of its interesting channel behavior, it has provided an important model for voltage-dependent conformational events in membrane proteins. However, alamethicin also provides a model for the study of membrane-protein interactions. The thermodynamics and lipid dependence of peptide-membrane binding have been examined for this peptide (Rizzo et al., 1987; Schwarz et al., 1986; Stankowski and Schwarz, 1989), and it demonstrates orientational changes in some systems as a function of hydration and lipid composition (Huang and Wu, 1991; He et al., 1996). In addition, alamethicin appears to modulate the membrane spontaneous curvature, and exhibits conductance states that are dependent upon the lateral stress in the bilayer (Keller et al., 1993; Keller et al., 1996). The energetics and structural requirements for the insertion of membrane-bound peptides is currently of considerable interest, as it has relevance to membrane protein biogenesis and the prediction of membrane protein structure (White and Wimley, 1994).

In lipid vesicle systems, structural studies on alamethicin indicate that it is inserted into the lipid bilayer, with the C-terminus of the peptide lying  $3\text{--}4 \text{ \AA}$  from the membrane-solution interface in the aqueous phase. Shown in Fig. 1 is a membrane structure for alamethicin that is consistent with recent NMR and electron paramagnetic resonance (EPR) data (Barranger-Mathys and Cafiso, 1996; Franklin et al., 1994). The majority of the peptide is already buried within the bilayer, and the energy price for moving the C-terminus across the membrane should be determined by the energy for moving the exposed C-terminus into the membrane hydrocarbon. For the structure shown in Fig. 1, the exposed C-terminal region consists of a C-terminal OH, Phe20, Gln19, and Gln18, and from the free energies of transfer for these three residues, a free energy of transfer of about +8 kcal/mol from water into hydrocarbon is obtained (Engleman et al., 1986). If the energy for burying three non-hydrogen-bonded C=O groups on the C-terminus is included, an energy barrier of about +14 kcal/mol is expected. There are approximately three hydrogen-bonded backbone pairs within the interfacial region of the bilayer, and recent calculations indicate that 2.2 kcal/mol would be associated with moving each of these pairs from solution into the membrane hydrocarbon (Ben-Tal et al., 1996). However, because these groups are already within the interface and the dielectric constant within this region is moderately low, the electrostatic energy required to bury these residues in the hydrophobic core is not expected to be significant. According to Eyring rate theory, the rate constant,  $k$ , should be described by  $k = (k_B T/h) \exp(-\Delta G^\ddagger/RT)$ , where  $k_B T/h$  is  $\sim 6 \times 10^{12} \text{ s}^{-1}$  at room temperature. A value of 14 kcal/mol for  $\Delta G^\ddagger$  yields a rapid transmembrane migration rate that is estimated to be  $\sim 200 \text{ s}^{-1}$ .

In planar bilayers, voltage-dependent conductances induced by alamethicin are often asymmetrical, such that a

Received for publication 14 November 1997 and in final form 17 February 1998.

Address reprint requests to Dr. David S. Cafiso, Department of Chemistry, University of Virginia, Charlottesville, VA 22901. Tel.: 804-924-3067; Fax: 804-924-3710; E-mail: cafiso@virginia.edu.

Dr. Franklin's present address is The Liposome Co., Princeton, NJ.

Dr. Barranger-Mathys's present address is Department of Chemistry, Mercyhurst College, Erie, PA.

© 1998 by the Biophysical Society

0006-3495/98/06/3023/08 \$2.00

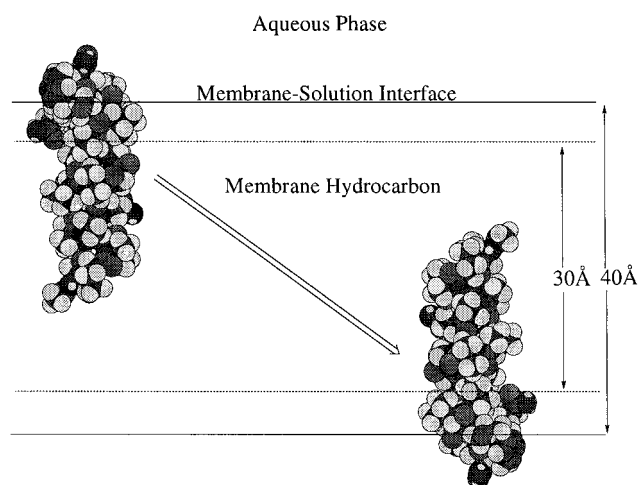


FIGURE 1 CPK model for placement of alamethicin in a lipid bilayer obtained from a combination of NMR and simulated annealing and site-directed spin labeling (Barranger-Mathys and Cafiso, 1996; Franklin et al., 1994). This figure depicts the transmembrane migration of the peptide C-terminus from one lipid vesicle monolayer to the other.

steeper logarithmic slope is usually seen for currents that are associated with *cis*-positive potentials rather than *cis*-negative potentials (the *cis* side of the bilayer is the side to which alamethicin is added). This asymmetry disappears when alamethicin is added to both sides of the planar bilayer, and it is presumed to result from an asymmetrical distribution of alamethicin across the bilayer (Vodyanoy et al., 1983). The extent of this asymmetry provides an indication of the transmembrane migration rate of the peptide across planar bilayers, and it is dependent upon the composition of the membrane, as well as the structure of the peptide (Hall et al., 1984; Vodyanoy et al., 1983). This approach provides a useful, although somewhat indirect method for gauging the transmembrane migration rate of alamethicin, and it indicates that transmembrane migration rates are relatively slow compared to the rates predicted based on the structure shown in Fig. 1. This discrepancy could be a result, in part, of the additional negative charge on the alamethicin analog used for the planar bilayer measurements, which contained glutamic acid at position 18. The additional charge at this position would be expected to add an additional 4.1 kcal/mol to the energy barrier.

Estimates of the transmembrane migration rate of alamethicin in lipid vesicles have not been made. The peptide structure in vesicles is reasonably well characterized, and the measured rates in these systems could be directly compared with free energy estimates for hydrophobic and electrostatic contributions to the partition energies of the peptide

C-terminus. In the present report, we examine the transmembrane movement of the C-terminus of alamethicin and an analog of alamethicin (L1) from one bilayer surface to the other. L1 is an analog of alamethicin in which MeA residues are replaced by Leu (see Table 1), which shows alamethicin-like activity in bilayers (Molle et al., 1989). The process depicted in Fig. 1 was examined by two independent methods based on NMR. In one approach, a spin-labeled analog of alamethicin was utilized in small unilamellar vesicles to produce paramagnetic line-broadening of the NMe proton resonances. In a second approach, the effect of unlabeled alamethicin on the  $^2\text{H}$  NMR quadrupole splitting was used to estimate the transmembrane migration rate in large unilamellar liposomes. Although both alamethicin and L1 are inserted into the lipid bilayer, their transmembrane migration rates are dramatically different. This difference parallels differences in the position of these two analogs along the bilayer normal.

## EXPERIMENTAL

### Materials

The spin labels 3-carboxyproxyl and 3-(aminomethyl)-proxyl were purchased from Sigma Chemical Co. (St. Louis, MO). Palmitoylcholine (POPC) was purchased as a chloroform solution from Avanti Polar Lipids (Alabaster, AL) and used without further purification. Alamethicin was obtained from Sigma Chemical Co. (St. Louis, MO), and the major fraction of alamethicin (having the sequence Ac-MeA-Pro-MeA-Ala-MeA-Ala-Gln-MeA-Val-MeA-Gly-Leu-MeA-Pro-Val-MeA-MeA-Gln-Gln-Phol, where MeA represents  $\alpha$ -methylalanine) was purified by high-performance liquid chromatography as described previously (Kelsh et al., 1992). A C-terminal spin-labeled analog of this derivative of alamethicin (Ala-Phol-SL) was prepared by forming an ester linkage between a 3-carboxyproxyl nitroxide and the C-terminal phenylalaninol, using a procedure described previously (Archer et al., 1991). The analog of alamethicin (L1), in which leucines replace each of the eight MeA residues (Molle et al., 1989), was created by solid-phase peptide synthesis and purified by high-performance liquid chromatography as described elsewhere (Barranger-Mathys and Cafiso, 1996). An analog of this peptide with a spin label on its C-terminus, L1-Phe-SL, was synthesized by coupling the aminomethyl-proxyl spin label through an amide linkage to the free C-terminus, as described previously (Barranger-Mathys and Cafiso, 1996). Cholesterol was obtained from Sigma Chemical Co. and used after recrystallization from ethanol. Octylglucoside was purchased from Aldrich Chemical Co. (Milwaukee, WI) and used without further purification. Deuterium oxide ( $\text{D}_2\text{O}$ ) was from Cambridge Isotope Laboratories (Woburn, MA).

## METHODS

### Synthesis of headgroup deuterated lipids

POPC selectively deuterated at the  $\alpha$  position of the choline headgroup was prepared as described previously (Marassi et al., 1993). The synthetic

TABLE 1 Sequences of alamethicin and L1

Peptide	Sequence*
Alam-Phol	Ac-MeA-Pro-MeA-Ala-MeA-Ala-Gln-MeA-Val-MeA-Gly-Leu-MeA-Pro-Val-MeA-MeA-Gln-Gln-Phol
L1	Ac-Leu-Pro-Leu-Ala-Leu-Ala-Gln-Leu-Val-Leu-Gly-Leu-Leu-Pro-Val-Leu-Leu-Gln-Gln-Phe

\*MeA is  $\alpha$ -methylalanine.

$\alpha$ -d<sub>2</sub>-POPC was purified by silica gel chromatography, and the purity of the product was checked by thin-layer chromatography and proton NMR.

### Preparation of lipid vesicles

To form sonicated vesicles, aliquots of POPC in chloroform were dried under a stream of nitrogen and vacuum desiccated for a minimum of 15 h at room temperature. The lipids were then dispersed in a 10 mM phosphate buffer formed in D<sub>2</sub>O (pD 7) at a total lipid concentration of ~100 mM. The lipid buffer dispersion was then ultrasonically irradiated at 0°C under a stream of argon and centrifuged to remove unsonicated lipid and titanium dust from the sonicator tip, following a procedure described previously (Castle and Hubbell, 1976). Giant unilamellar vesicles (GUVs) were produced from a solution of octylglucoside and lipid (70 mol%  $\alpha$ -d<sub>2</sub>-POPC, 30 mol% cholesterol in 10 mM HEPES, 150 mM NaCl, pH 7.0) as described previously (Marassi et al., 1993). Before the NMR measurements were made, aliquots of alamethicin, L1, or their spin-labeled analogs were added from concentrated solutions in methanol and extensively vortexed to produce membrane concentrations ranging from less than 1 mol% to 20 mol% peptide.

### NMR spectroscopy

Proton NMR spectra of sonicated vesicles were obtained with a 500-MHz GE Omega spectrometer using a standard one pulse sequence for protons. Transformed spectra were fitted to Lorentzian lineshapes and analyzed using the NMR analysis software package FELIX, version 2.3 (San Diego, CA). Deuterium NMR spectra were obtained for headgroup-labeled GUVs using a highly modified Nicolet NT-360 NMR spectrometer operating at a frequency of 55.1 MHz and equipped with a wide-line <sup>2</sup>H solids probe (Cryomagnetics Systems, Indianapolis, IN). A quadrupole echo-pulse sequence was used to acquire the spectra (Davis et al., 1976), with 90° pulses of ~3  $\mu$ s duration, a recycle delay of 1.5 s, and an exponential line-broadening of 50 Hz. Procedures suggested previously were followed to ensure that Fourier transformation was started at the top of the spin echo (Rance and Byrd, 1983), and no first-order phase corrections were used. The <sup>2</sup>H NMR spectra were typically the result of ~25,000 acquisitions.

## RESULTS

### Transmembrane migration of paramagnetic amphiphiles can be monitored using <sup>1</sup>H NMR

Shown in Fig. 2 *A* is an expansion of the proton NMR spectrum of small, sonicated lipid vesicles (SUVs), which includes the *N*-methyl (NMe) resonance. In these vesicles, two NMe resonances are seen as a result of packing differences between the internal and external vesicle monolayers, and have previously been well documented for these vesicle systems (Huang and Mason, 1978; Xu and Cafiso, 1986). In the present case, the exterior and interior resonances are observed to have intrinsic linewidths of ~4 and ~7 Hz, respectively. Shown in Fig. 2 *B* is the NMe resonance after the addition of the spin-labeled alkylamide I (see Scheme 1) to the vesicle suspension. This label is completely membrane-associated under the conditions used here, and it is known to be freely membrane permeable (Cafiso and Hubbell, 1978). Although the changes in linewidth are more pronounced on the internal monolayer, probe I produces linewidth changes in both the internal and external NMe resonances. For example, at a very low membrane probe concentration of 0.03 mol%, probe I produces linewidth

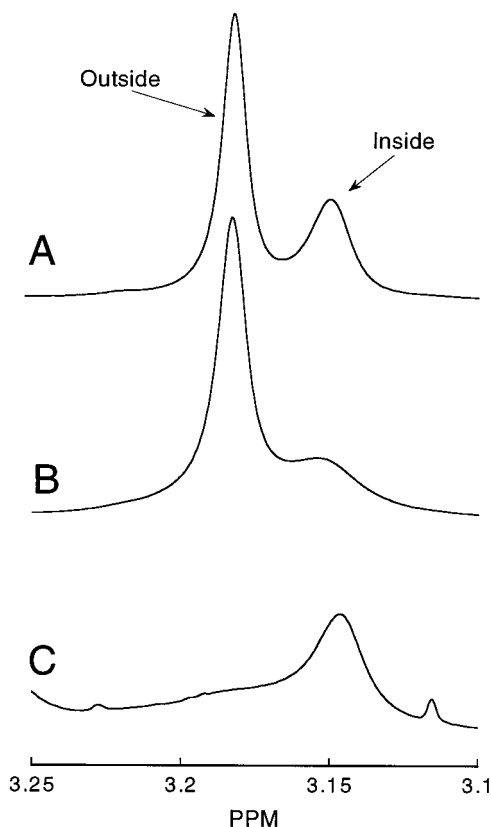
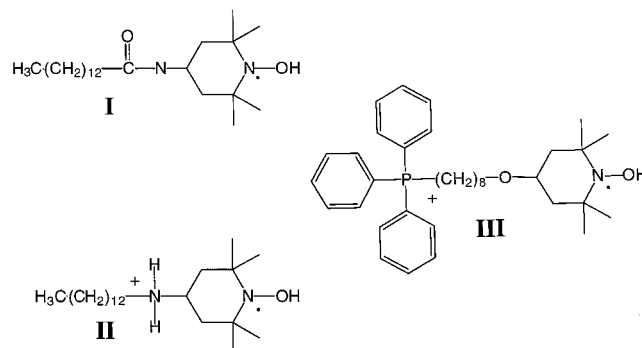


FIGURE 2 (*A*) Proton NMR spectrum of sonicated POPC vesicles, showing the interior and exterior NMe resonances. (*B*) Spectrum in the presence of the alkylamide spin-label I at a probe-to-lipid ratio of 0.12 mol%. (*C*) Spectrum of the NMe resonance in the presence of alkylammonium II at a probe-to-lipid ratio of 2 mol%. For all three vesicle samples, the spectra were recorded at 25°C in a D<sub>2</sub>O buffer containing 10 mM sodium phosphate, pD 7.0, at a total lipid concentration of 10 mM.

increases of  $1.36 \pm 0.33$  and  $4.62 \pm 36$  Hz in the internal and external NMe resonances, respectively. Nitroxides are well known to produce increases in the spin-spin relaxation rates for nearby protons (Morrisett, 1976), and the increases in linewidth on both surfaces are consistent with the changes expected for a membrane-permeable probe.

Whereas probe I is uncharged and membrane permeable, the alkylammonium probe II is known to be relatively



SCHEME 1

impermeable in these vesicle systems (Castle and Hubbell, 1976). Shown in Fig. 2 *C* is a  $^1\text{H}$  NMR spectrum showing the NMe resonance of sonicated vesicles after the addition of II to the vesicle suspension. In contrast to probe I, significant linewidth increases are seen only for the external NMe resonance. For example, at a membrane-bound concentration of 0.48 mol%, probe II produces a linewidth increase of  $8.97 \pm 0.81$  Hz in the external NMe resonance, but no significant change in the internal resonance. Both nitroxide probes I and II lie within the membrane interface (Ellena et al., 1988), and these results are consistent with the expectation that I is highly permeable, whereas II is impermeable on the time scale of the experiment.

In addition to these two probes, we also used  $^1\text{H}$  NMR to follow the migration rate of a paramagnetic hydrophobic ion, III, which strongly associates with the membrane, but is known to migrate across the bilayer under the influence of a transmembrane potential (Cafiso and Hubbell, 1981, 1982). Fig. 3 shows a plot of the linewidths of the internal and external NMe resonance after the creation of a pH gradient when 200  $\mu\text{M}$  of the alkylphosphonium nitroxide, III, is added to the vesicle exterior. After the establishment of an inside acidic pH gradient, an inside negative transmembrane potential develops in these membranes within 20–40 min, as an electrochemical equilibrium is established (Perkins and Cafiso, 1987). As seen in Fig. 3, after the creation of a pH gradient, the external linewidth decreases and the internal linewidth increases on a time scale that is consistent with the establishment of a membrane potential in these systems. These changes in linewidth are consistent with an increase in the nitroxide concentration on the internal monolayer, and a concomitant decrease in concentration

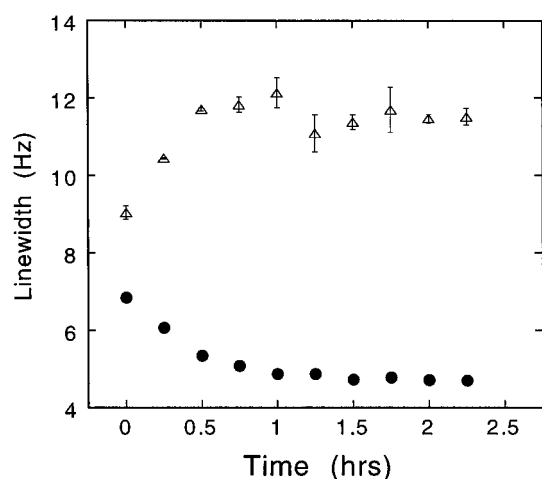


FIGURE 3 The effect of 200  $\mu\text{M}$  C8 phosphonium label on the internal ( $\Delta$ ) and external ( $\bullet$ ) proton NMR linewidths of sonicated vesicles formed from POPC as a function of time after the creation of a pH gradient. The lipid concentration was  $\sim 60$  mM, and the buffer contained 125 mM  $\text{Na}_2\text{SO}_4$  and 100 mM NaPhos. The internal pH was 7.0, and the external pH was adjusted to 10 at  $t = 0$ . These vesicles develop a transmembrane potential that comes to equilibrium with  $\Delta\text{pH}$ , resulting in transmembrane migration of the phosphonium label.

on the external monolayer resulting from the establishment of an inside negative potential. These observations provide a strong indication that paramagnetic broadening of the  $^1\text{H}$  NMe resonances provides a reasonable method of measuring the transmembrane migration of a membrane-associated spin label.

### The transmembrane migration of alamethicin is very slow across lipid vesicles

Shown in Fig. 4 *B* is the proton NMR spectrum of the NMe resonance after the addition of 200  $\mu\text{M}$  C-terminal spin-labeled alamethicin analog (Ala-Phol-SL). The relative amplitudes of these two resonances are now dramatically different and are a result of changes in the linewidth of the external NMe resonance. Fig. 5 *A* shows a plot of the linewidth changes for both the internal and external resonances as a function of peptide concentration. Whereas there is more than a twofold increase in the external NMe linewidth upon the addition of 200  $\mu\text{M}$  Ala-Phol-SL, there is no significant change in the linewidth of the internal NMe resonance, even at the highest concentrations of peptide. The linewidths of the interior and exterior lipid NMe reso-

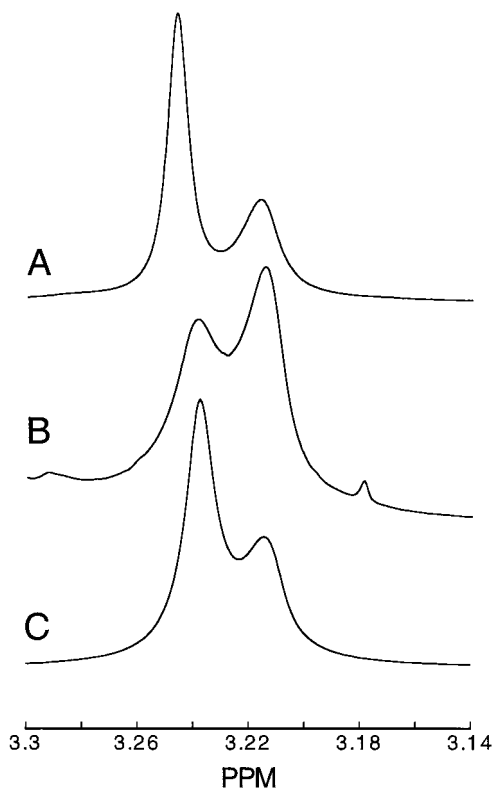


FIGURE 4 (*A*) Proton NMR spectrum of sonicated POPC vesicles, showing the interior and exterior NMe resonances. (*B*) NMe resonance for sonicated vesicles after the addition of Alamethicin to a vesicle sample at a peptide:lipid molar ratio of 1:300. (*C*) NMe resonance after the addition of the leucine analog, L1-Phe-SL, to a vesicle sample at a peptide:lipid molar ratio of 1:317. These spectra were recorded at 25°C, using a vesicle sample with a total lipid concentration of 59 mM in a  $\text{D}_2\text{O}$  buffer of 10 mM sodium phosphate (pD 7.0).



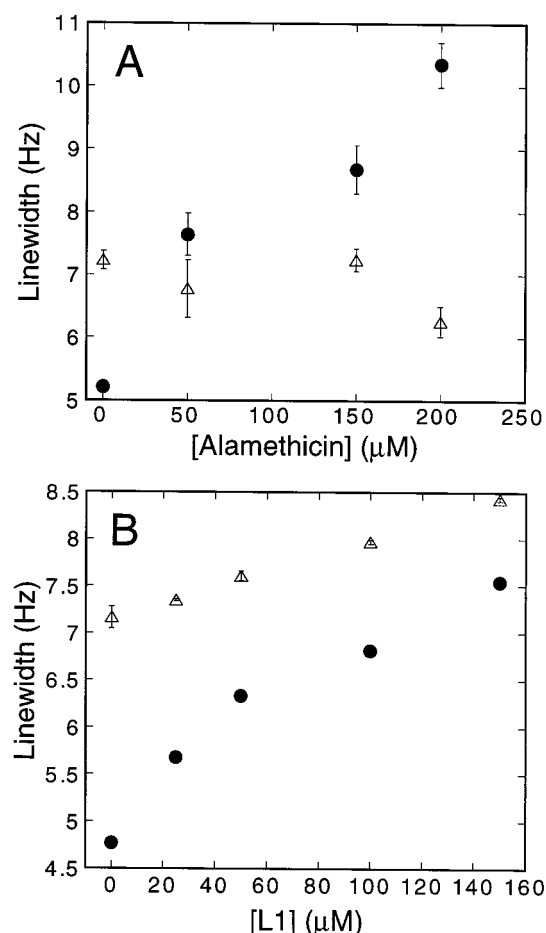


FIGURE 5 Internal ( $\Delta$ ) and external ( $\bullet$ ) linewidths for the  $^1\text{H}$  NMR resonances of sonicated unilamellar vesicles of POPC as a function of the concentration of added (A) Ala-Phol-SL or (B) L1-Phe-SL at  $25^\circ\text{C}$ . Vesicles were at a concentration of 59 mM in a  $\text{D}_2\text{O}$  buffer of 10 mM sodium phosphate (pD 7.0).

nances were followed for a period of over 50 h, and no further changes in the internal or external linewidths were detected during this period. It should be noted that the highest membrane concentration used here corresponds to a peptide:lipid ratio of 1:200, and the observed effect on external linewidth is clearly quite sensitive to addition of the spin-labeled peptide. These changes are a result of paramagnetic enhancements in the spin-spin relaxation rate, and no change in either the internal or external linewidth was seen when non-spin-labeled, native alamethicin was added to POPC vesicles under these same concentrations. These data, when combined with the observations on simple amphiphiles, provide a strong indication that the nitroxide on alamethicin resides only on the external monolayer, and that alamethicin does not cross from the outer to the inner membrane surface in these model membranes. Based on the uncertainty in the linewidths, the transmembrane migration rate for alamethicin in these model membrane systems is estimated to be no greater than  $1 \times 10^{-4} \text{ min}^{-1}$ .

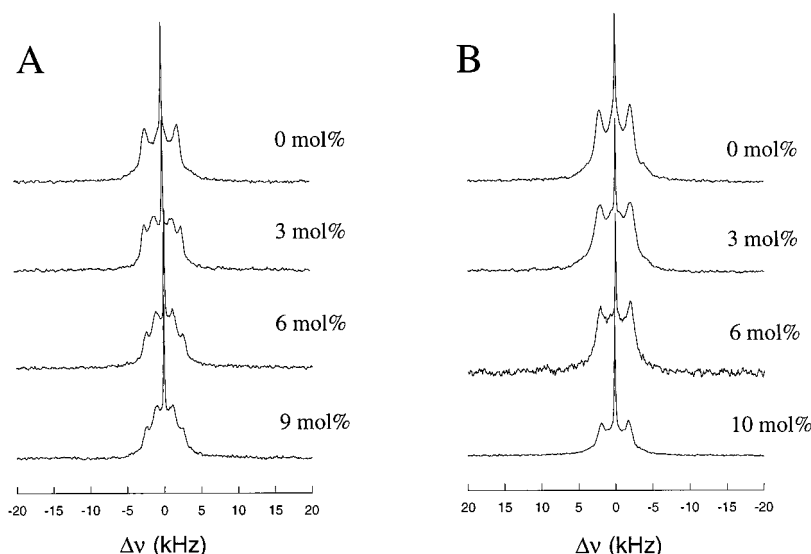
Because these vesicles are small and are known to be highly strained, it is conceivable that the apparent lack of

migration is a result of packing differences between the internal and external monolayers. To test for this possibility, the migration rate was examined for native (non-spin-labeled) alamethicin in giant unilamellar vesicles (GUVs) using  $^2\text{H}$  NMR. Previous work has shown that the interaction of peptides with each monolayer of the GUV can be detected by using  $^2\text{H}$  NMR or  $^{31}\text{P}$  NMR (de Kroon et al., 1991; Marassi et al., 1993). Shown in Fig. 6 A are a series of  $^2\text{H}$  NMR spectra as a function of increasing alamethicin concentration in GUVs formed with phosphatidylcholine deuterated in the  $\alpha$  choline position of the lipid headgroup. Addition of alamethicin to the external vesicle solution leads to  $^2\text{H}$  spectra consisting of two pake patterns. One pake pattern has a quadrupolar splitting of  $\sim 5$  kHz and is similar to that measured in the absence of alamethicin, and the second pake pattern has a narrower splitting of  $\sim 3$  kHz. Whereas the concentration of alamethicin does not effect the broader pake pattern, the quadrupolar splitting of the narrow component is seen to decrease as a function of the externally added alamethicin concentration and is only 1.8 kHz at 12 mol% alamethicin. The ratio of the lipid populations contributing to the two pake patterns, which was determined by subtracting the spectrum in the absence of peptide from a two-component spectrum, is  $\sim 1:1$  and was unaffected by the alamethicin concentration. The appearance of two pake patterns with a 1:1 intensity ratio after the addition of alamethicin is consistent with the peptide interacting with only one (exterior) monolayer of the GUVs. (The  $^2\text{H}$  NMR spectra that are obtained in the presence of alamethicin show two pake patterns, and this has been taken to indicate that alamethicin interacts with one monolayer of the GUVs. The pake pattern with a narrower quadrupolar splitting most likely reflects the increased headgroup motion of the lipids that are interacting with alamethicin. It should be noted that the appearance of two pake patterns is not inconsistent with the inserted orientation for alamethicin shown in Fig. 1. In this structure, the N-terminus of the peptide does not extend into the headgroup region of the opposite monolayer, and addition of alamethicin would not necessarily be expected to perturb the interior lipid headgroups and the quadrupolar splitting of resonances from the inner monolayer.) The  $^2\text{H}$  spectra of GUVs in the presence of alamethicin were monitored over minimum period of 10 h, and no changes in the spectra were observed. This result is consistent with the previous result suggesting that spin-labeled alamethicin is quite impermeable across sonicated unilamellar membranes in the absence of a potential. Thus the conclusions reached are qualitatively similar to those obtained in sonicated vesicles and suggest that neither the size of the vesicle nor the presence of the spin label have a significant effect on the migration rate of this peptide.

#### The L1 analog of alamethicin migrates rapidly across lipid bilayers

Shown in Fig. 4 C is the proton NMR spectrum obtained after the addition of the spin-labeled MeA alamethicin an-

FIGURE 6 (A)  $^2\text{H}$  NMR spectra of giant unilamellar vesicles (GUVs) formed from a mixture of POPC/cholesterol (70:30) as a function of increasing amounts of alamethicin. The spectra, top to bottom, correspond to spectra at 0, 3, 6, and 9 mol% alamethicin, respectively. The total lipid concentration in these samples was 77 mM. (B)  $^2\text{H}$  NMR spectra of GUVs formed from a mixture of POPC/cholesterol (70:30) in the presence of externally added L1. The spectra, top to bottom, correspond to membrane concentrations of L1 of 0, 3, 6, and 10 mol%, respectively. The total lipid concentration in these samples was 77 mM.



alog, L1-Phe-SL. For this sample, L1-Phe-SL was found to produce line broadening in both the internal and external NMe signals of 1.7 and 2.2 Hz, respectively. Fig. 5 B shows the effect of spin-labeled L1 on the linewidths of the external and internal NMe resonances as a function of concentration. Unlike alamethicin, L1-Phe-SL increased linewidths for both the internal and external surfaces. The native non-labeled peptide L1 did not produce line broadening in either of the NMe resonances, indicating that the observed effects are paramagnetic in origin. The changes in line broadening for L1-Phe-SL were observed immediately after the addition of the peptide, and no further changes in the internal linewidth were detected. Because the spin label on the C-terminus can only produce relaxation of the internal resonance if it gains access to the internal surface, this peptide must rapidly migrate across the vesicle membrane. Thus, in contrast to the behavior of alamethicin, this analog appears to be at equilibrium across the vesicle membrane during the time scale of this experiment. The migration of this more hydrophobic analog was also examined by using  $^2\text{H}$  NMR. Shown in Fig. 6 B are a series of  $^2\text{H}$  NMR spectra after the addition of L1. In the presence of the L1 analog, only one peak pattern is seen, and the quadrupolar splitting was observed to decrease with increasing L1 concentration from 4.2 kHz in the absence of L1 to 3.2 kHz in the presence of 13 mol% L1. The extent of incorporation of L1 into these bilayers was checked by examining the interaction between the spin-labeled L1 analog L1-Phe-SL and extruded lipid vesicles (1000-Å diameter, 70:30 PC:cholesterol). The EPR spectrum of the L1 analog in the presence of vesicles was highly anisotropic under conditions similar to those used above for the  $^2\text{H}$  NMR experiments, and was similar to that obtained previously for membrane-bound L1. Previous work demonstrated that under the conditions used here, L1 efficiently incorporates into the vesicle membrane (Barranger-Mathys and Cafiso, 1996). Thus, in contrast to alamethicin, which appears to interact only on the external

vesicle surface, the analog L1 interacts with both surfaces of the bilayer. L1 comes to equilibrium across the bilayer within the time period required to accumulate the  $^1\text{H}$  NMR data ( $\sim 2$  min). Given the uncertainty in these measurements, the migration rate of L1 is estimated to be at least  $0.5 \text{ min}^{-1}$  or at least three orders of magnitude greater than the migration of native alamethicin.

### Effects of temperature

The spin-labeled peptides Ala-Phol-SL and L1-Phe-SL were studied at both elevated and lowered temperatures, respectively, in an attempt to resolve the kinetics of their transmembrane migration. When the NMe linewidths in POPC vesicles were monitored at an elevated temperature of  $50^\circ\text{C}$ , no evidence for changes in the internal linewidth or for a transmembrane migration of Ala-Phol-SL could be detected. When L1-Phe-SL was examined at a depressed temperature of  $7^\circ\text{C}$ , both NMe resonances were immediately broadened, and no resolution of the kinetics of migration (as was seen for probe III) could be detected. Using a simple Eyring rate analysis, the lack of migration of Ala-Phol-SL at  $50^\circ\text{C}$  reflects an energy barrier that is greater than 29 kcal/mol, whereas for L1-Phe-SL the lower limit of the estimated rate at  $7^\circ\text{C}$  corresponds to a barrier of  $\sim 19$  kcal/mol. Thus the energy differences in the barrier for the transmembrane migration of Ala-Phol-SL versus L1-Phe-SL appear to be 10 kcal/mol or greater.

### DISCUSSION

The data obtained here demonstrate that the transmembrane distribution of spin-labeled amphiphiles and peptides can be followed in small lipid vesicles by measuring the paramagnetic enhancement produced by a nitroxide on the spin-spin relaxation rate of the *N*-methyl phospholipid protons. Mea-

measurements on spin-labeled derivatives of alamethicin and L1 indicate that whereas alamethicin remains trapped on one membrane interface in the absence of a potential, L1 is able to rapidly cross bilayers. This conclusion is also consistent with the effects of unlabeled alamethicin or L1 on the  $^2\text{H}$  NMR linewidths of the phospholipid headgroup in GUVs.

The limits that these measurements place on the transport of alamethicin and L1 across bilayers raise several interesting questions. For example, why is alamethicin trapped on one surface? A rough estimate of the size of the energy barrier for the transit of this peptide can be made based on the membrane structure (Fig. 1) and the transfer free energies for the side chains and groups in the exposed C-terminal domain. This yields an energy barrier of  $\sim 14$  kcal/mol, which should permit a rapid transmembrane migration at normal temperatures. (For the  $^1\text{H}$  NMR measurements made here that employ a spin-labeled analog of alamethicin, the expected energy barrier for the transmembrane migration of alamethicin should in fact be less than 14 kcal/mol, because of the additional hydrophobicity of the nitroxide label and the acetylation at the peptide C-terminus.) However, the data obtained here indicate that this estimate is 10–15 kcal/mol less than that actually encountered. At the present time, the interactions leading to this additional energy are not understood. Clearly, because the N-terminus and most of the peptide are buried within the membrane hydrocarbon, the C-terminal domain of the peptide must be the source for this energy. Additional energy barriers to transport might arise from hydrogen-bonding interactions between the peptide backbone and the membrane lipid or solvent. Such interactions would not be expected to be strong for a purely  $\alpha$ -helical structure, but might occur for an irregular helix; and indeed, there is evidence that alamethicin is an irregular helix at its C-terminus (Franklin et al., 1994). In addition to these interactions, some steric interactions would be encountered as the peptide is moved through the membrane hydrocarbon; however, because the membrane hydrocarbon is a liquid, it is difficult to imagine that this could account for the additional energy barrier seen here.

Another interesting question raised by the measurements made here is the source of the remarkably different rates for the transmembrane migration of alamethicin versus L1. This difference reflects a difference in the energy barrier for translocation that is on the order of 10 kcal/mol or larger. In addition to this difference in kinetics, alamethicin and L1 appear to take up different positions in the bilayer. Shown in Fig. 7 are the approximate positions of alamethicin and L1 within the membrane interface, as determined by collision gradient EPR spectroscopy (Barranger-Mathys and Cafiso, 1996). In these membranes, both alamethicin and L1 are monomeric. L1 is translocated  $\sim 3$ – $4$  Å deeper into the bilayer interface compared to alamethicin, and its C-terminus is buried within the interface, in contrast to the C-terminus of alamethicin. One explanation for the differing positions is the additional hydrophobicity of L1 versus alamethicin, and conceivably, this hydrophobicity might

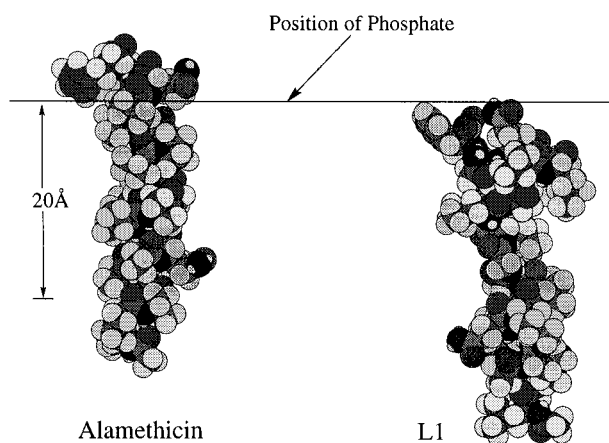


FIGURE 7 Membrane structures of alamethicin and L1 relative to the membrane interface. The structure of alamethicin was determined from  $^1\text{H}$  NMR in detergent micelles (Franklin et al., 1994), and the placement of the peptides along the bilayer normal was determined using site-directed spin labeling and collision gradient EPR (Barranger-Mathys and Cafiso, 1996). The structure of L1 shown was obtained from a simulated annealing of NMR data obtained from detergent micelles (Jacob and Cafiso, unpublished observations).

also account for the faster migration rate of L1. If alamethicin is prevented from migrating because of hydrogen bond interactions within the interface, a faster migration of L1 could result if the energy price for overcoming these hydrogen bond interactions were paid for by the additional hydrophobicity of L1. However, only two MeA residues in alamethicin, at positions 16 and 17, are not already buried within the membrane hydrocarbon. Based on their accessible surface areas in a helix, substituting these residues with leucine should not add more than  $\sim 2$  kcal/mol to the free energy of transfer. Given that the difference in the energy barrier between these two peptides is on the order of 10 kcal/mol, it appears unlikely that the additional hydrophobicity at these two positions can account for the differences in their transmembrane migration rate. In light of this quantitative discrepancy, a more likely explanation for the differences in migration rate is simply that the structures for the two peptides are different within the membrane interface. Structural data that confirm this latter possibility are not currently available.

Evidence for the transmembrane migration rate of several other peptides has been obtained. For example, the signal sequence from cytochrome oxidase IV (CoxIV) contains several positively charged residues, and it has been found to migrate across model membranes containing POPC and phosphatidylglycerol on the time scale of minutes (Maduke and Roise, 1993). It has been reported that the translocation of magainin 2, a positively charged peptide at physiological pH, is coupled to pore formation (Matsuzaki et al., 1995). The lack of migration of alamethicin is remarkable in comparison, considering that it is uncharged and much more hydrophobic than either the CoxIV signal sequence or magainin. This difference likely reflects the presence of acid

lipids, which appear to interact strongly with these basic peptides, and may themselves participate in the transport.

In summary, alamethicin transits lipid bilayers much more slowly than is expected based on the expected transfer free energy of its C-terminus. L1, an analog of alamethicin in which MeA is replaced by Leu, transits bilayers with a rate that is at least three orders of magnitude faster than that of alamethicin. A likely explanation for this result is that the backbone of alamethicin interacts strongly within the membrane interface, whereas the analog L1 does not. The results obtained here suggest that features other than side-chain hydrophobicity play an important role in determining the energy barriers to peptide and protein transport across membranes.

This research was supported by a grant from the National Institutes of Health (GM-35215) to DSC.

## REFERENCES

- Archer, S. J., J. F. Ellena, and D. S. Cafiso. 1991. Dynamics and aggregation of the peptide ion channel alamethicin. *Biophys. J.* 60:389–398.
- Barranger-Mathys, M., and D. S. Cafiso. 1996. Membrane structure of voltage-gated channel forming peptides revealed by site-directed spin labeling. *Biochemistry*. 35:498–505.
- Ben-Tal, N., A. Ben-Shaul, A. Nicholls, and B. Honig. 1996. Free-energy determinants of  $\alpha$ -helix insertion into lipid bilayers. *Biophys. J.* 70:1803–1812.
- Cafiso, D. S. 1994. Alamethicin: a peptide model for voltage-gating and protein membrane electrostatic interactions. *Annu. Rev. Biophys. Biomol. Struct.* 23:141–165.
- Cafiso, D. S., and W. L. Hubbell. 1978. Estimation of transmembrane pH gradients from phase equilibria of spin-labeled amines. *Biochemistry*. 17:3871–3877.
- Cafiso, D. S., and W. L. Hubbell. 1981. EPR determination of membrane potentials. *Annu. Rev. Biophys. Bioeng.* 10:217–244.
- Cafiso, D. S., and W. L. Hubbell. 1982. Transmembrane electrical currents of spin-labeled hydrophobic ions. *Biophys. J.* 39:263–272.
- Castle, J. D., and W. L. Hubbell. 1976. Estimation of membrane surface potential and charge density from the phase equilibrium of a paramagnetic amphiphile. *Biochemistry*. 15:4818–4831.
- Davis, J. H., K. R. Jeffrey, M. Bloom, M. I. Valic, and T. P. Higgs. 1976. Quadrupolar echo deuterium magnetic resonance spectroscopy in ordered hydrocarbon chains. *Chem. Phys. Lett.* 42:390–394.
- de Kroon, A., J. A. Killian, J. de Geir, and D. Kruijff. 1991. The membrane interaction of amphiphilic model peptides affects phosphatidylserine headgroup and acyl chain order and dynamics. Application of the “phospholipid headgroup electrometer” concept to phosphatidylserine. *Biochemistry*. 30:1155–1162.
- Ellena, J. F., S. J. Archer, R. N. Dominey, B. D. Hill, and D. S. Cafiso. 1988. Localizing the nitroxide group of fatty acid and voltage sensitive spin-labels in phospholipid bilayers. *Biochim. Biophys. Acta*. 940:63–70.
- Engleman, D. M., T. A. Steitz, and A. Goldman. 1986. Identifying non-polar transbilayer helices in amino acid sequences of membrane proteins. *Annu. Rev. Biophys. Biophys. Chem.* 15:321–353.
- Franklin, J. C., J. F. Ellena, S. Jayasinghe, L. P. Kelsh, and D. S. Cafiso. 1994. The structure of micelle associated alamethicin from  $^1\text{H}$  NMR. Evidence for conformational heterogeneity in a voltage-gated peptide. *Biochemistry*. 33:4036–4045.
- Hall, J. E., I. Vodyanoy, T. M. Balasubramanian, and G. R. Marshall. 1984. Alamethicin: a rich model for channel behavior. *Biophys. J.* 45:233–247.
- He, K., S. J. Ludtke, W. T. Heller, and H. W. Huang. 1996. Mechanism of alamethicin insertion into lipid bilayers. *Biophys. J.* 71:2669–2679.
- Huang, C., and J. T. Mason. 1978. Geometric packing constraints in egg phosphatidylcholine vesicles. *Proc. Natl. Acad. Sci. USA*. 75:308–310.
- Huang, H. W., and Y. Wu. 1991. Lipid-alamethicin interactions influence alamethicin orientation. *Biophys. J.* 60:1079–1087.
- Keller, S. L., S. M. Bezrukov, S. M. Gruner, M. W. Tate, I. Vodyanoy, and V. A. Parsegian. 1993. Probability of alamethicin conductance states varies with nonlamellar tendency of bilayer phospholipids. *Biophys. J.* 65:23–27.
- Keller, S. L., S. M. Gruner, and K. Gawrisch. 1996. Small concentrations of alamethicin induce a cubic phase in bulk phosphatidylethanolamine mixtures. *Biochim. Biophys. Acta*. 1278:241–246.
- Kelsh, L. P., J. F. Ellena, and D. S. Cafiso. 1992. Determination of the molecular dynamics of alamethicin using  $^{13}\text{C}$  NMR: implications for the mechanism of gating of a voltage-dependent channel. *Biochemistry*. 31:5136–5144.
- Latorre, R., and O. Alvarez. 1981. Voltage-dependent channels in planar lipid bilayer membranes. *Physiol. Rev.* 61:77–150.
- Maduke, M., and D. Roise. 1993. Import of a mitochondrial presequence into protein-free phospholipid vesicles. *Nature*. 260:364–367.
- Marassi, F. M., R. R. Shivers, and P. M. Macdonald. 1993. Resolving the two monolayers of a lipid bilayer in giant unilamellar vesicles using deuterium magnetic resonance. *Biochemistry*. 32:9936–9943.
- Mathew, M. K., and P. Balaram. 1983. Alamethicin and related membrane channel forming polypeptides. *Mol. Cell. Biochem.* 50:47–64.
- Matsuzaki, K., O. Murase, N. Fujii, and K. Miyajima. 1995. Translocation of a channel forming antimicrobial peptide, magainin 2, across lipid bilayers by forming a pore. *Biochemistry*. 34:6521–6526.
- Molle, G., H. Dulozier, J. Y. Dugast, and G. Spach. 1989. Design and conformation of non-Aib synthetic peptides enjoying alamethicin-like ionophore activity. *Biopolymers*. 28:273–283.
- Morrisett, J. D. 1976. The use of spin labels for studying the structure and function of enzymes. In *Spin Labeling, Theory and Applications*. Academic Press, New York. 273–338.
- Perkins, W. R., and D. S. Cafiso. 1987. Characterization of  $\text{H}^+/\text{OH}^-$  currents in phospholipid vesicles. *J. Bioenerg. Biomembr.* 19:443–455.
- Rance, H., and A. Byrd. 1983. Obtaining high-fidelity spin-1/2 powder spectra in anisotropic media: phase-cycled Hahn echo spectroscopy. *J. Magn. Reson.* 52:221–240.
- Rizzo, V., S. Stankowski, and G. Schwarz. 1987. Alamethicin incorporation in lipid bilayers: a thermodynamic analysis. *Biochemistry*. 26:2751–2759.
- Sansom, M. S. P. 1993. Alamethicin and related peptaibols—model ion channels. *Eur. Biophys. J.* 22:105–124.
- Schwarz, G., S. Stankowski, and V. Rizzo. 1986. Thermodynamic analysis of incorporation and aggregation in a membrane: application to the pore forming peptide alamethicin. *Biochim. Biophys. Acta*. 861:141–151.
- Stankowski, S., and G. Schwarz. 1989. Lipid dependence of peptide-membrane interactions. Bilayer affinity and aggregation of the peptide alamethicin. *FEBS Lett.* 250:556–560.
- Vodyanoy, I., J. E. Hall, and T. M. Balasubramanian. 1983. Alamethicin-induced current-voltage curve asymmetry in lipid bilayers. *Biophys. J.* 42:71–82.
- White, S., and W. C. Wimley. 1994. Peptides in lipid bilayers: structural and thermodynamic basis for partitioning and folding. *Curr. Opin. Struct. Biol.* 4:79–86.
- Woolley, G. A., and B. A. Wallace. 1992. Model ion channels: gramicidin and alamethicin. *J. Membr. Biol.* 129:109–136.
- Xu, Z.-C., and D. S. Cafiso. 1986. Phospholipid packing and conformation in small vesicles revealed by two-dimensional  $^1\text{H}$  nuclear magnetic resonance cross-relaxation spectroscopy. *Biophys. J.* 49:799–783.